Biomedical Letters ISSN 2410-955X– An International Biannually Journal

Research article
2020 | Volume 6 | Issue 1 | Pages 60-67

ARTICLE INFO

Received
January 08, 2020
Revised
March 21, 2020
Accepted
May 05, 2020

***Corresponding Author**
Jianli Wang

E-mail
jianli@uow.edu.au

Keywords
ZnO
Nanospheres
Hydrothermal process
Glioblastoma Multiforme
Anticancer

How to Cite
Iqbal Y, Mustafa MK, Wang J, Wang C, Majeed U, Muhammad P, Rehman FU. Synthesis and growth mechanism of ZnO nanospheres by hydrothermal process and their anticancer effect against glioblastoma multiforme. Biomedical Letters 2020; 6(1):60-67.

Scan QR code to see this publication on your mobile device.

Special Issue: Nanotechnology in Nanomedicine

Open Access

Synthesis and growth mechanism of ZnO nanospheres by hydrothermal process and their anticancer effect against glioblastoma multiforme

Younas Iqbal[1], Mohd Kamarulzaki Mustafa[2], Jianli Wang[1,4], Chao Wang[1], Uzair Majeed[3], Pir Muhammad[5], Fawad Ur Rehman[5], Imtiaz Ahmad[6]

[1]Institute for Computational Materials Science, School of Physics and Electronics, Henan University, Kaifeng, 475004, china
[2]Department of Physics and Chemistry, Faculty of Applied Sciences and Technology, Universiti Tun Hussein Onn Malaysia, Educational Hub Pagoh, 84000, Muar, Johor, Malaysia
[3]Department of Physics NED university of engineering and technology, Karachi
[4]Institute for Superconducting & Electronic Materials, University of Wollongong
[5]International Joint Center for Biomedical Innovation, School of Life Sciences, Henan University, Kaifeng, Henan 475004, China
[6]College of Chemistry and Molicular Engineering, Zhengzhou University, Zhengzhou, 450001, China

Abstract

Glioblastoma Multiforme (GBM) is one of the fatal cancers, primarily affecting the brain. Currently, no complete treatment is available. Nanotechnology-based approaches have the potential to meet this challenge. In this contribution, single-crystalline ZnO nanoparticles were synthesized by the hydrothermal method and employed in biomedicine as GBM ablating agent. Various concentrations of precursors, Zinc Nitrate Hexahydrate {($Zn(NO_3)_2.6H_2O$)} and Hexamethylene Tetraamine ($C_6H_{12}N_4$) were mixed after vigorous stirring at the same temperature and deposition time. The resultant nanoparticles were characterized through field emission scanning electron microscopy FESEM (7699F, Japan) for surface microstructure, energy dispersive x-ray spectroscopy EDX (7699F, Japan) for elemental composition and X-rays diffraction XRD (Xpert^3, PAN alytical, USA) for crystalline structure respectively. This technique was used for the first time to synthesized ZnO nanoparticles. The largest particle size calculated at 0.5 mM is 84.8721 A^o. Moreover, the GBM cells (LNZ-308) showed excellent uptake, whereas DCFDA analysis for reactive oxygen species (ROS) generation data revealed significantly higher yield as compared to PBS. Besides, the MTT assay showed the excellent anticancer effect of ZnO nanoparticles treatment (up to 80 %) after 24 hours of incubation. These results suggest unique nano ZnO spheres excellent biomedical applications for GBM resection.

Introduction

Brain cancers are fatal among all other kinds of diseases [1]. Glioblastoma Multiforme (GBM) is comprised of 60 % of all diagnosed brain cancers, with a median survival rate of below 15 months after diagnosis [2]. Annually 330,000 cases of brain cancers are reported all around the world, and among countries, China is top-ranked in terms of brain cancer provenance [3]. The temozolomide is only available GBM ablating drug. However, its application can only increase the median survival to several months [4]. Therefore a facile, robust, and cost-effective treatment for GBM resection is highly desired [5].

The research on nanomaterial has been more prominent in various scientific fields since the last several decades due to its fascinating and fanciful properties in practical applications [6, 7]. ZnO is one of the most important semiconducting material with many nanostructures and can be used in various practical applications, including biomedicine. Amongst the nanospheres of ZnO is a unique nanostructure formed by linking multiple nanoparticles with single-crystalline and large specific surface area [8]. Due to the large surface area, phototoxic effect and versatile surface chemistry, the ZnO nanomaterials are universally applicable in drug delivery and bioimaging. Moreover, the US food and drug administration (FDA) has graded ZnO as "GRAS" (generally recognized as safe) substance and is potentially applicable in biomedical applications [9]. The research on ZnO nanomaterials demonstrates that it can accomplish reactive oxygen species (ROS) on reacting with cell membrane lipids and show surpassing toxicity against the cancer cells [10].
The research studies show that the combination of ZnO nanoparticles forms ZnO nanoparticles. Many techniques such as chemical vapor deposition and layer-by-layer were used to produce hollow nanospheres [11]. Electrochemical method was used in the presence of polyatomic ion POMs (polyoxometalates) at room temperature to obtain ZnO nanoparticles. It is experimentally demonstrated that these ions POMs has a crucial role in the fabrication of ZnO nanoparticles [12]. Bakrudeen *et al*., [13] synthesized the self-induced fluorescence mesoporous (order porous) ZnO nanoparticles for the drug delivery of pharmaceutical drug towards the magnamented disorder condition [14].

Ching *et al*. [15] produced ZnO nanoparticles through evaporation of NH_3 by using ammonium hydroxide (NH_4OH) and $Zn(NO_3)_2$ as starting precursors . Qian et al. [16] synthesized steady nanoparticles, comprising of tightly stuffed nanoparticles shells with a shell wall thickness of a few tens of nanometers by the controlled precipitation of metal cations with urea in the presence carbonaceous saccharide nanospheres as hard templates. Erbium Er^{3+} doped ZnO nanoparticles were produced by using $Zn(NO_3)_26H_2O$, triethanolamine (TEA) and $Er(NO_3)_3.5H_2O$ as precursors, and a sufficient improvement in photoluminescence intensity was observed. Yonh [17] used ZnO nanoparticles with the particle size of 10 nm for dye-sensitized solar cells (DSSC), prepared from diethylene glycol (DEC) and zinc acetate dehydrate (ZnAc), and observed an increase in light to electricity conversion efficiency (0.474% - 1.03%) as compared to nanoparticle-based DSSC.
In the present study, a novel technique is introduced to produce ZnO nanoparticles from various precursor concentrations, and its effect on surface morphology (Microstructure), crystalline structure, and micro composition is investigated. Moreover, the prepared nanostructures were further applied for the Glioblastoma Multiforme (GBM) resection in vitro, as biomedical applications.

Materials and Methods

Materials

The premium glass microscope slides (fisher scientific) were used as substrate and were coated with chromium and gold Cr (20) nm- Au (50) nm as adhesive and seed layer respectively. The chemicals zinc nitrate hexahydrate $Zn(NO_3)_2.6H_2O$ and hexamethylene tetraamine ($C_6H_{12}N_4$) were purchased from Sigma-Aldrich were dissolved in de-ionized (DI) water with a conductivity of 18 Ω/cm^2. Thermo Fisher provided all the cell culture media and chemicals, whereas the nest biotechnologies (Wuxi, China) flasks were used for cell culture

Substrate Cleaning

The premium glass microscope slides were ultrasonically rinsed in acetone and in DI water respectively for 10 minutes before use to remove the contaminants. A Cr (20) nm-Au (50) nm seed layer was deposited on an ultrasonically rinsed glass

substrate using double target sputter coater Quorun model (Q300TD) for the heterogeneous nucleation.

Hydrothermal growth and nucleation

An equimolar (0.4-0.9) mM solution of $Zn(NO_3)_2.6H_2O$ and $C_6H_{12}N_4$ were prepared independently each in 50 ml high resistivity Milli-Q DI water using magnetic bar stirrer overnight and then mixed together. The ZnO nanoparticles are synthesized by submerging the Cr-Au seeded substrate inside the precursor and is kept in preheated oven for 6 hours at 90 ˚C. The samples are rinsed with DI water for 1 minute and then dried in an ambient environment. The resultant nano ZnO spheres were characterized by FESEM (Field emission scanning electron microscope JEOL JSM-7600F), EDX (electron dispersive x-ray spectroscopy, JEOL JSM-7600F) and XRD (X-ray diffraction, X,pert^3 powder in the 2θ range of 10°-80°) for microstructure, elemental composition and crystal structure respectively.

Cell culture

The LNZ-308 cells were provided by the Joint Center for Biomedical innovations, Henan University and were cultured in DMEM with 10% FBS and 1% Streptomycin-Penicillin solution. The cells were incubated under standard culture conditions i.e., 37^{o}C temperature, with 95% humidity in the presence of 5% CO_2.

MTT assay

The MTT assay was performed by culturing the 1x10^3 LNZ-308 cells in 96 well plates for 24 hours under standard culturing conditions. Then various concentrations of ZnO nanoparticles (i.e. 15, 30, 40, 45, 50, 55, 60 and 0 µM) were inoculated for further 24 hours. Afterward, the 10 µl of 5mg/mL MTT assays solution was added to each well and further incubated for 4 hours. The supernatant was then removed and 200 µL of dimethyl sulfoxide DMSO was added to each well and incubated for 10 minutes. The optical density read at 492 nm wavelength and data was analyzed via the following formula;

$$\text{Viability (\%)} = \frac{OD\ of\ treated\ cells}{OD\ of\ nontreated\ cells} x100$$

Cell uptake

For cell uptake of ZnO nanoparticles, the LNZ-308 cells were cultured in a specialized confocal Petri dishes and were treated with ZnO nanoparticles tagged with FITC as reported earlier and were incubated for overnight. Then the cell nucleus was stained with DAPI for 5 minutes and fixed with 4% paraformaldehyde solution for 10 minutes. The samples were then analyzed under a confocal scanning microscope (Zeiss LSM 800).

ROS evaluation

The cells were cultured in the same manner as for uptake and then treated with ZnO nanoparticles for 24 hours. The DCFDA solution was added to the samples and was further incubated for 30 minutes. Then the cells were imaged under a confocal scanning microscope at 488 nm wavelength. The fluorescence intensity was directly proportional to the number of reactive oxygen species (ROS) generated.

Results and Discussion

As prepared ZnO Nanoparticles Characterization

The FESEM images of ZnO nanoparticles reveals that all the substrates are decorated with ZnO nanoparticles as shown in **Fig. 1**. The FESEM images show that these nanostructures are formed by the aggregation of individual nanoparticles. No linear changes in shape and size of nanoparticles were observed with a change in concentration, as both small and large size nanoparticles can be seen in all samples. There is no considerable change in the morphology of the nanoparticles, presented in **Fig. 1 A, B, C, D, E** and **F**. The density of the nanoparticles has increased with an increase in concentration up to 0.8 mM, whereas a further increase in level i.e., 0. 9 mM, the increase in the size of nanoparticles was observed as shown in **Fig. 1 F**.

From EDX spectra, both Zn and O are detected (**Fig. 2**). The small peaks at positions ~ 1.7 and ~2.1 represent gold (Au) from the substrate coated with the gold seed layer before deposition. A nonlinear relationship in percent atomic ratio of constituent atoms Zn and O is observed in all concentrations as shown in **Table 1**. The schematic of the growth process of ZnO nanoparticles is shown in **Fig. 3**, in which $Zn(NO_3)_26H_2O$ and $C_6H_{12}N_4$ decompose and produce an intermediate compound $Zn(OH)_2$. The OH- group of $Zn(OH)_2$ react with neighbor $Zn(OH)_2$ and developed a linkage between them. The ZnO nanoparticles are produced by the dehydration of $Zn(OH)_2$ and accumulated to form a spherically shaped structure by Ostwald ripening process to

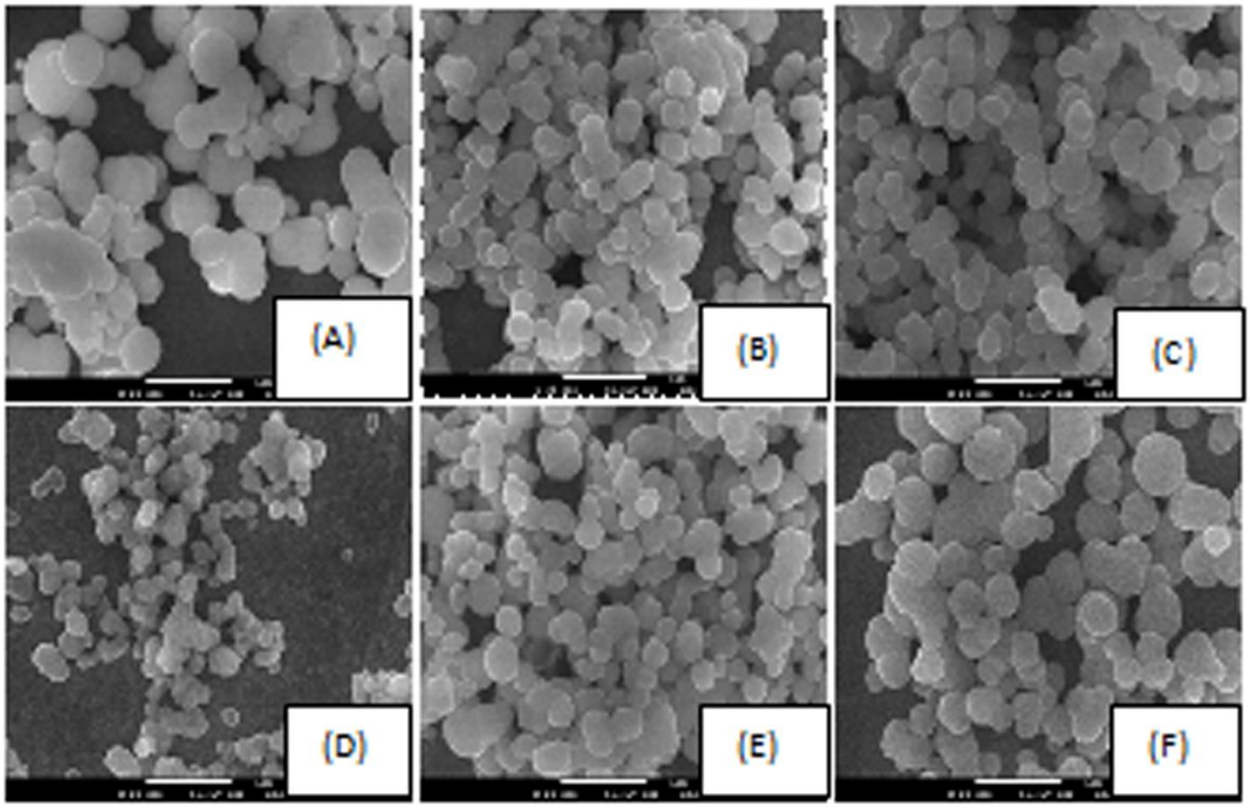

Fig. 1: Typical FESEM images of prepared spherical ZnO nanoparticles at various concentrations of 0.4 mM(A) 0.5 mM (B) 0.6 mM(C) 0.7 mM(D) 0.8 mM(E) 0.9 mM(F). The scalebar is 1 µm.

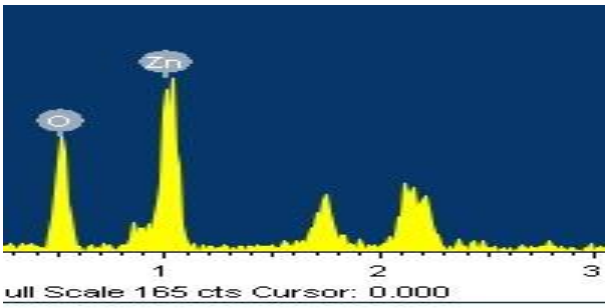

Fig. 2: The EDX spectra of ZnO nanoparticles

reduce the cluster surface energy [18]. During the creation of ZnO nanoparticles, the nanoparticles with different charges produced by the dehydration of $Zn(OH)_2$ develop a dipole and tends to minimize its electrical potential and surface energy.

XRD analysis is used to investigate the phase and crystal structure of the synthesized ZnO nanoparticles as shown in **Fig. 4**. The XRD pattern shows that all the samples consist of hexagonal structure of ZnO except 0.7 mM and 0.9 mM which represent wurtzite and cubic crystal structure respectively. There is no characteristic peak for the intermediate nuclei $(Zn(OH)_2$ is observed, reveals the pure phase of ZnO nanoparticles. There is a broad peak at 38° in XRD pattern for all concentrations of pure ZnO nanoparticles along with some additional peaks at 10^o, 20^o and 20^o, 30^o in 0.4 mM only. The XRD pattern of 0.5 mM and 0.9 mM is almost the same except for an additional peak in 0.5 mM, which may be due to the difference in crystalline structure and lattice parameters, as shown in **Table 2**.The broadening of peaks reveals the full width at half maximum (FWHM) β and can be used to calculate the size of the particle in synthesized ZnO nanoparticles by using Debye-Scherrer formula given as:

$$D = \frac{k\lambda}{\beta cos\theta} \qquad (1)$$

Table 1: percent composition of Zn and O obtained by EDX at various concentrations

No	Conc. (mM)	Atomic(Zn)	Percentage (O)
1	0.4	27.6400	72.3600
2	0.5	29.9900	70.0100
3	0.6	27.7000	72.3000
4	0.7	23.2200	76.7800
5	0.8	26.6600	73.3400
6	0.9	27.0800	72.9200

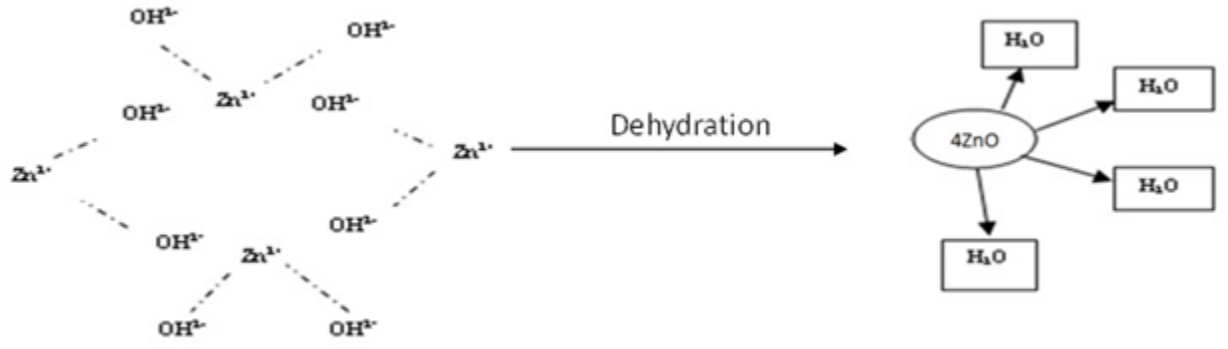

Fig. 3: Schematic drawing of the formation of ZnO nanoparticles

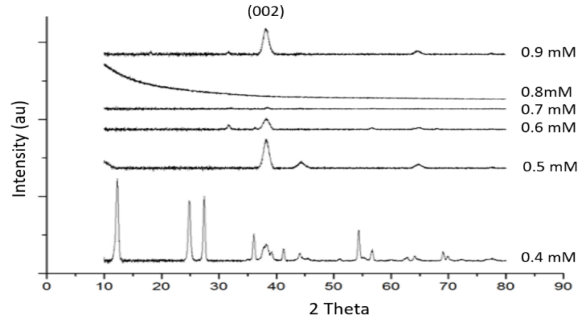

Fig. 4. XRD study of ZnO nanoparticles at various concentrations

Table 2: Lattice parameters (a, b and c) and crystalline structure of nanoparticle in ZnO nanoparticles

No	Conc. (mM)	Crystalline structure	Density (g/cm^3)	a (Å)	b (Å)	c (Å)
1	0.4	Hexagonal	3.48	5.33	5.33	6.15
2	0.5	Hexagonal	5.65	3.25	3.25	5.22
	0.6	Hexagonal	5.67	5.25	5.25	5.20
4	0.7	wurtzite	6.04	3.17	3.17	5.12
5	0.8	Amorphous				
6	3	cubic	5.67	4.62	4.62	4.62

Where λ and β are the wavelength, and full width at half maximum (FWHM) of the diffraction peaks respectively and k=0.89 (Scherrer's constant). The FWHM of only (002) peaks of all concentrations is used for the particle size calculation. The values of lattice parameters a, b, and c obtained from XRD results are given in **Table 3**.

Table 3: Particle size of ZnO nanoparticle in individual nanoparticles.

No	Conc. (mM)	FWHM	2θ	Particle size (D) Å
1	0.4	0.1085	16.70	25.6559
2	0.5	0.1574	17.16	84.8721
3	0.6	0.3936	16.00	13.9402
4	0.7	0.4961	18.66	3.09882
5	0.8			
6	0.9	0.2755	19.00	5.542782

Anticancer effect

After characterization, we employed the as-prepared ZnO nanoparticles for GBM resection as biomedical applications. The Zn is well tolerated by our body, as it is already listed as one of the essential minerals of our body, helping in physiology and homeostasis maintenance, and regulates cellular enzymes [19]. Moreover, its role in immunity and anti-stress is also well known [20]. Therefore, ZnO based nanoparticles have inherited biocompatibility and inertness to our body as compared to other nanoscale formulations [21].

The uptake study showed excellent ZnO nanoparticles interaction with cells and was easily untaken by the GBM cells (**Fig. 5**). We observed that at lower concentration, the ZnO nanoparticles were inert and had no considerable toxic effect; however, at higher concentration, the ZnO nanoparticles could produce the cytotoxic impact as shown in **Fig. 6**. The GBM cytotoxic effect was concentration dependent i.e., at 60 µM, around 80 percent cytotoxicity was observed. Meanwhile, the lower concertation of 15 µM could only induce 15% cell mortality. It is well known that all the metallic nanoparticles can produce reactive oxygen species, especially the ZnO, which is well reported for its anticancer and antibacterial effects [22-24]. Recently, Rauf et al. biosynthesized bougainvillea scaffold-based nanoscale ZnO that had both antibacterial and anti-cancer activity [25]. Similarly, Shobha et al. reported bio-fabricated ZnO with anticancer and antifungal properties [26].

In our study, we used DCFDA as a ROS detection dye to further confirms the ZnO nanoparticles potential of ROS generation. We observed that after 24 hours inoculation in GBM cells, the ZnO nanoparticles could produce a significantly higher amount of ROS as compared to the control (**Fig. 7**).

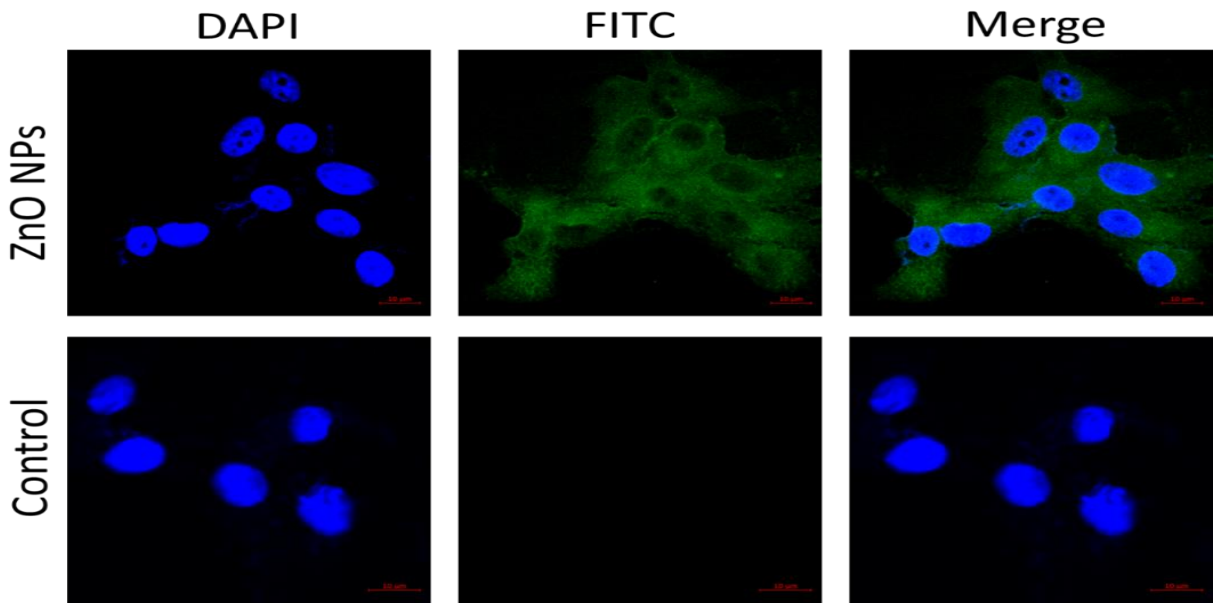

Fig. 5: Cell uptake of ZnO nanoparticles after tagging with FITC as a standard dye. The cell nucleus is stained with DAPI.

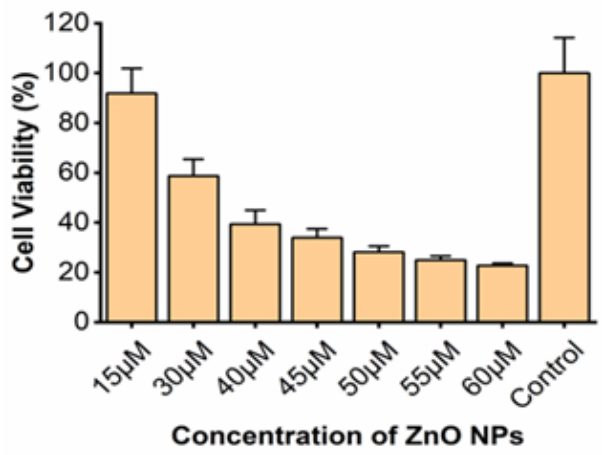

Fig. 6: GBM cells viability after treatment with ZnO NPs.

The ROS are essential mediators of cell functionality and signal transduction at the optimum level and needed for proper cell physiology. However, the increase in ROS level e.g., OH^-, O_2, H_2O_2 can induce oxidative stress that in turn, leads to cell apoptosis [27, 28]. Herein, the as-prepared ZnO nanoparticles concentration dependent cell cytotoxicity of GBM is evident that increased concentration of ZnO leads to an elevated level of ROS that induces the apoptosis. The cancer cell biology is different from the health cells i.e. higher in NADP(H), ROS, GSH-GSSG (glutathione) and lower in pH i.e. ~5.5-6.5 [29]. In such a condition's further revelation of ROS level by the employment of metal nanoparticles e.g. ZnO, break the threshold level of ROS tolerance and induce intracellular apoptosis.

Conclusion

A single step, simple, and economical solution-based method is designed to synthesize solid ZnO nanoparticles. The effect of different concentrations on the surface microstructure, crystal structure of the ZnO nanosphere is addressed. An appropriate growth mechanism based on the chemical reaction during the growth process is presented. The ZnO nanoparticles were reported for the first time through this method. Besides, the as prepared ZnO has an excellent anticancer effect against GBM by producing a higher level of ROS in a dose-dependent manner. This modality based fabricated ZnO is facile, cost-effective and has the potential of biomedical applications.

Acknowledgments

The authors are grateful to the center for graduate studies, University Tun Hussein Onn Malaysia, and ministry of education, Malaysia, for the financial supporting this research through graduate researcher incentive grant (GIPS) project vote U058.

Conflict of interest

The authors declare no conflict of interest.

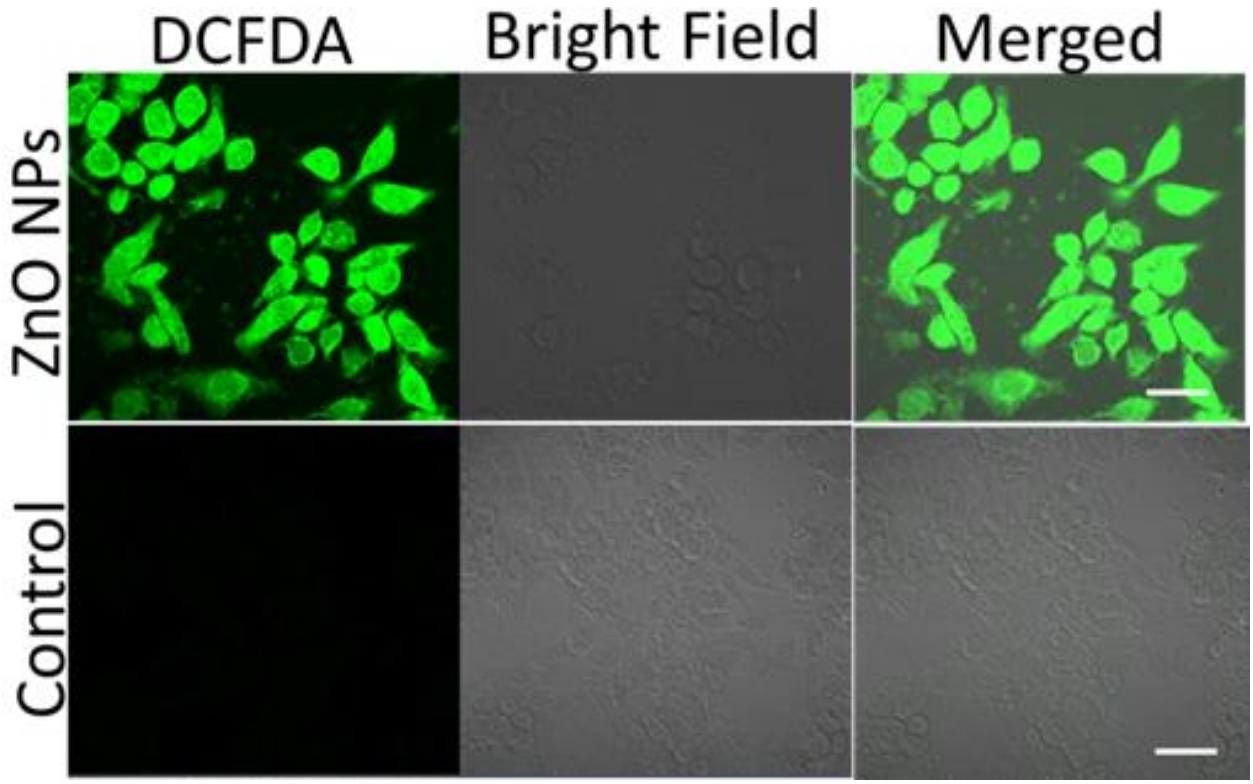

Fig. 7: ROS generation by GBM cells after Treatment with ZnO NPs. The scale bar is 50 µM.

References

[1] Sanai N, Alvarez-Buylla A, Berger MS. Neural stem cells and the origin of gliomas. New England Journal of Medicine. 2005;353:811-22.

[2] Srikanth M, Kessler JA. Nanotechnology—novel therapeutics for CNS disorders. Nature Reviews Neurology. 2012;8:307.

[3] Patel AP, Fisher JL, Nichols E, Abd-Allah F, Abdela J, Abdelalim A, et al. Global, regional, and national burden of brain and other CNS cancer, 1990–2016: a systematic analysis for the Global Burden of Disease Study 2016. The Lancet Neurology. 2019;18:376-93.

[4] Mrugala MM, Chamberlain MC. Mechanisms of disease: temozolomide and glioblastoma—look to the future. Nature Reviews Clinical Oncology. 2008;5:476.

[5] Shi J, Kantoff PW, Wooster R, Farokhzad OC. Cancer nanomedicine: progress, challenges and opportunities. Nature Reviews Cancer. 2017;17:20.

[6] Smith AM, Nie S. Semiconductor nanocrystals: structure, properties, and band gap engineering. Accounts of chemical research. 2009;43:190-200.

[7] Devan RS, Patil RA, Lin JH, Ma YR. One-Dimensional Metal-Oxide Nanostructures: Recent Developments in Synthesis, Characterization, and Applications. Advanced Functional Materials. 2012;22:3326-70.

[8] Yang C, Li Q, Tang L, Bai A, Song H, Yu Y. Monodispersed colloidal zinc oxide nanospheres with various size scales: synthesis, formation mechanism, and enhanced photocatalytic activity. Journal of Materials Science. 2016;51:5445-59.

[9] Jiang J, Pi J, Cai J. The Advancing of Zinc Oxide Nanoparticles for Biomedical Applications. Bioinorganic Chemistry and Applications. 2018;2018:18.

[10] Moezzi A, McDonagh AM, Cortie MB. Zinc oxide particles: Synthesis, properties and applications. Chemical Engineering Journal. 2012;185-186:1-22.

[11] Wang SL, Jia X, Jiang P, Fang H, Tang WH. Large-scale preparation of chestnut-like ZnO and Zn–ZnO hollow nanostructures by chemical vapor deposition. Journal of Alloys and Compounds. 2010;502:118-22.

[12] Kołodziejczak-Radzimska A, Jesionowski T. Zinc Oxide—From Synthesis to Application: A Review. Materials. 2014;7:2833-81.

[13] Bakrudeen HB, Sugunalakshmi M, Reddy BSR. Auto-fluorescent mesoporous ZnO nanospheres for drug delivery carrier application. Mater Sci Eng C Mater Biol Appl. 2015;56:335-40.

[14] Spanhel L, Anderson MA. Semiconductor clusters in the sol-gel process: quantized aggregation, gelation, and crystal growth in concentrated zinc oxide colloids. Journal of the American Chemical Society. 1991;113:2826-33.

[15] Cheng L, Zheng L, Li G, Yin Q, Jiang K. Synthesis of sealed sponge ZnO nanospheres through a novel NH3-evaporation method. Nanotechnology. 2008;19:075605.

[16] Qian H, Lin G, Zhang Y, Gunawan P, Xu R. A new approach to synthesize uniform metal oxide hollow nanospheres via controlled precipitation. Nanotechnology. 2007;18:355602.
[17] Zhang Y, Wu L, Liu Y, Xie E. Improvements to the hierarchically structured ZnO nanosphere based dye-sensitized solar cells. Journal of Physics D: Applied Physics. 2009;42:085105.
[18] Layek A, Mishra G, Sharma A, Spasova M, Dhar S, Chowdhury A, et al. A Generalized Three-Stage Mechanism of ZnO Nanoparticle Formation in Homogeneous Liquid Medium. The Journal of Physical Chemistry C. 2012;116:24757-69.
[19] Murakami M, Hirano T. Intracellular zinc homeostasis and zinc signaling. Cancer science. 2008;99:1515-22.
[20] Rink L, Haase H. Zinc homeostasis and immunity. Trends in immunology. 2007;28:1-4.
[21] Hambidge KM, Miller LV, Westcott JE, Sheng X, Krebs NF. Zinc bioavailability and homeostasis. The American journal of clinical nutrition. 2010;91:1478S-83S.
[22] Mishra PK, Mishra H, Ekielski A, Talegaonkar S, Vaidya B. Zinc oxide nanoparticles: a promising nanomaterial for biomedical applications. Drug discovery today. 2017;22:1825-34.
[23] Lai L, Jiang X, Han S, Zhao C, Du T, Rehman FU, et al. In vivo biosynthesized zinc and iron oxide nanoclusters for high spatiotemporal dual-modality bioimaging of Alzheimer's disease. Langmuir. 2017;33:9018-24.
[24] Jana TK, Jana SK, Kumar A, De K, Maiti R, Mandal AK, et al. The antibacterial and anticancer properties of zinc oxide coated iron oxide nanotextured composites. Colloids and Surfaces B: Biointerfaces. 2019;177:512-9.
[25] Rauf MA, Oves M, Rehman FU, Khan AR, Husain N. Bougainvillea flower extract mediated zinc oxide's nanomaterials for antimicrobial and anticancer activity. Biomedicine & Pharmacotherapy. 2019;116:108983.
[26] Shobha N, Nanda N, Giresha AS, Manjappa P, Sophiya P, Dharmappa K, et al. Synthesis and characterization of Zinc oxide nanoparticles utilizing seed source of Ricinus communis and study of its antioxidant, antifungal and anticancer activity. Materials Science and Engineering: C. 2019;97:842-50.
[27] Rehman FU, Zhao C, Jiang H, Selke M, Wang X. Protective effect of TiO2 nanowhiskers on Tetra Sulphonatophenyl Porphyrin (TSPP) complexes induced oxidative stress during photodynamic therapy. Photodiagnosis Photodyn Ther. 2016;13:267-75.
[28] Christopher SF. Type I and Type II Mechanisms of Photodynamic Action. Light-Activated Pesticides: American Chemical Society; 1987. p. 22-38.
[29] Rehman FU, Jiang H, Selke M, Wang X. Mammalian cells: a unique scaffold for in situ biosynthesis of metallic nanomaterials and biomedical applications. Journal of Materials Chemistry B. 2018;6:6501-14.